IEEE Access
Multidisciplinary | Rapid Review | Open Access Journal

Received October 21, 2021, accepted December 2, 2021, date of publication December 10, 2021,
date of current version December 23, 2021.

*Digital Object Identifier 10.1109/ACCESS.2021.3134252*

# Design of a Patch Power Divider With Simple Structure and Ultra-Broadband Harmonics Suppression

**SAEED ROSHANI[1], (Member, IEEE), SLAWOMIR KOZIEL[2,3], (Senior Member, IEEE), SOBHAN ROSHANI[1], MOHAMMAD (BEHDAD) JAMSHIDI[4,5], (Member, IEEE), FARIBORZ PARANDIN[1], AND STANISLAW SZCZEPANSKI[3]**

[1]Department of Electrical Engineering, Kermanshah Branch, Islamic Azad University, Kermanshah, Iran
[2]Department of Engineering, Reykjavik University, 102 Reykjavik, Iceland
[3]Faculty of Electronics, Telecommunications and Informatics, Gdansk University of Technology, 80-233 Gdansk, Poland
[4]Research and Innovation Centre for Electrical Engineering, University of West Bohemia, 301 00 Pilsen, Czech Republic
[5]Department of Power Electronics and Machines (KEV), University of West Bohemia, 301 00 Pilsen, Czech Republic

Corresponding author: Sobhan Roshani (s.roshani@aut.ac.ir)

This work was supported in part by the Icelandic Centre for Research (RANNIS) under Grant 206606, and in part by the National Science Centre of Poland under Grant 2018/31/B/ST7/02369.

**ABSTRACT** This paper introduces a simple H-shaped patch Wilkinson power divider (WPD), which provides ultra wide harmonics suppression band. The presented WPD designed at 1.8 GHz, and exhibits good performance at the operating bandwidth. In the proposed divider structure, two simple patch low-pass filters (LPFs) are employed at each branch, and three open ended stubs are added at each port. The proposed divider, implemented using the aforementioned structures has a good performance at both higher frequencies, and the operating frequency. In particular, the designed divider provides an ultra wide suppression band from 3 GHz to 20 GHz, which encompasses the 2$^{nd}$ up to the 11$^{th}$ harmonic. The proposed WPD has an operating band from 1.62 GHz to 2.1 GHz, with the operating bandwidth exceeding 480 MHz. Consequently, the fractional bandwidth (FBW) of 25.8 percent is obtained. The results indicate $|S_{11}|$, $|S_{12}|$, $|S_{22}|$, and $|S_{23}|$, are equal to $-17$ dB, $-3.5$ dB, $-20$ dB, and $-17$ dB, respectively, at the operating frequency. The simulation results are corroborated through the measurements of the fabricated divider prototype. The superior harmonic suppression capability is also demonstrated through comparisons with state-of-the-art divider circuits from the literature.

**INDEX TERMS** Resonator, harmonics suppression, patch power divider, patch resonator.

## I. INTRODUCTION

The dividers belong to popular components in microwave circuits and systems. A conventional Wilkinson divider exhibits good performance at its operating frequency, yet it transmits unwelcome harmonics along with the main signal without any suppression, which is undesirable in many applications [1]. Consequently, design of modified dividers with harmonics elimination has become an important design consideration in modern communication systems. Some of available methods introduced to suppress unwanted harmonics are outlined below. In [2]–[6], harmonic elimination has been achieved by means of electromagnetic bandgap (EBG) cells. This approach has been demonstrated effective but needs additional steps in both the design and the fabrication processes, thereby making it difficult to implement. In a number of works, e.g., [7]–[12], defected ground structures have been used to realize harmonics canceling. The defected ground methods prove suitable for the purpose yet—similarly as EBG—additional design and fabrication steps are required, which is a downside.

In many designs, lumped reactive components, such as inductors and capacitors [13]–[19], are applied to provide wide harmonics elimination range. On the other hand, while the usage of lumped components is effective for harmonics suppression, it limits the operating frequency and increases the losses at higher frequencies.

Open-ended and short-ended stubs also are widely used to suppress unwanted harmonics in dividers [20]–[26]. These techniques allow for simple structures and planar designs. However, a single stub only suppresses a single harmonic,

The associate editor coordinating the review of this manuscript and approving it for publication was Wenjie Feng.

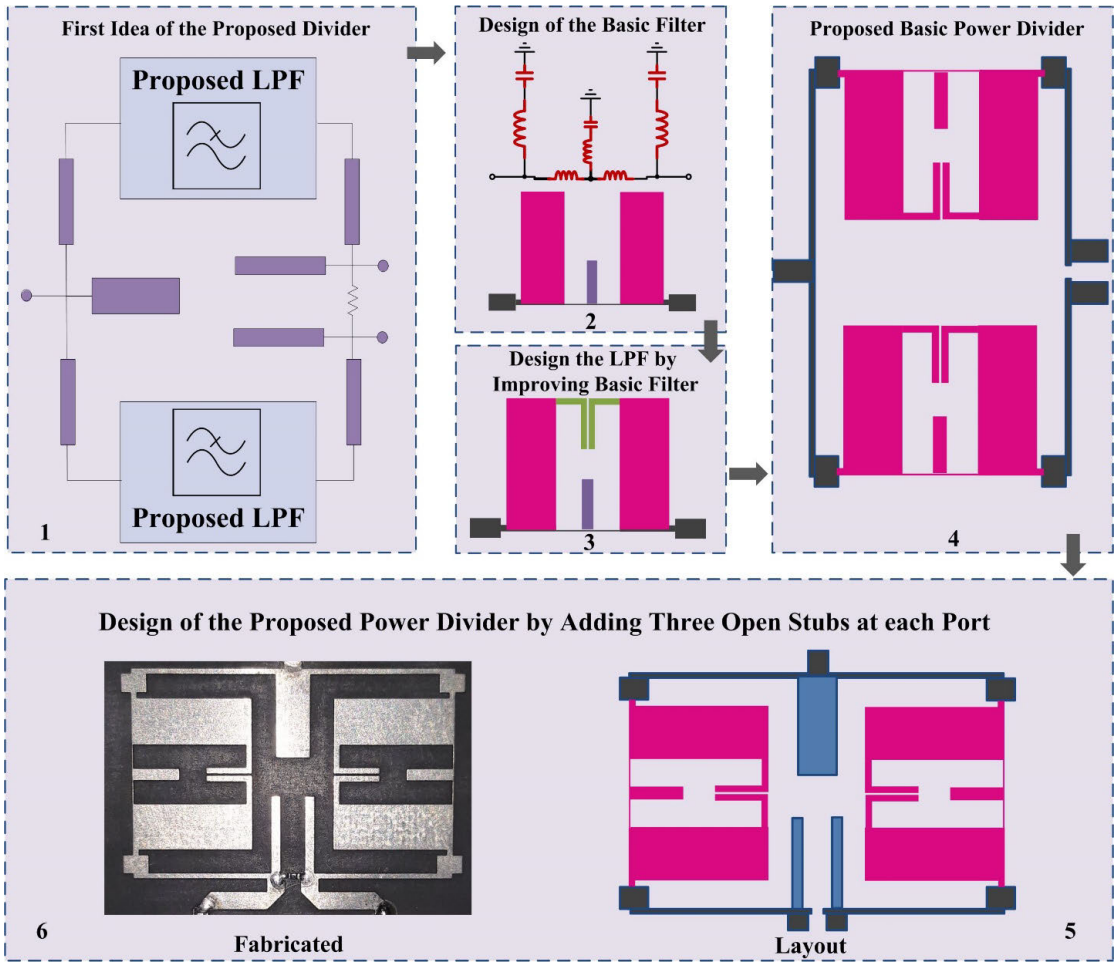


**FIGURE 1.** Design procedure of the proposed power divider. The design process is graphically illustrated in steps 1 through 6. Step 1 shows the circuit model, whereas steps 2 to 5 present the subsequent stages of the development of the divider circuit, including layouts of different parts of the structure. Also, step 6 shows the fabricated divider prototype. In the figure, different colors refer to different resonators and circuit components.

therefore, to implement a broad harmonic suppression band, several stubs have to be used, which increases the circuit complexity. Yet another approach to harmonics cancelling are power dividers based on coupled line architectures [27]–[32]. Coupled lines provide bandpass responses and eliminate unwanted harmonics, but suffer from high insertion losses in the passband. Perhaps the most common method to reduce harmonics in the divider structures is utilization of resonators. Several dividers have been reported in the literature with different types of resonators to suppress unwanted harmonics [33]–[43]. Resonators are effective in suppressing of unwanted harmonics, but also contribute to insertion losses, which increase the overall insertion loss of the divider. In terms of algorithmic approaches, artificial intelligence methods, which has been widely used to solve engineering problems [44]–[51], can be employed to modeling and design of power dividers [52], [53].

Recently, patch structures have become popular in the design of microwave devices, examples including patch resonators, patch filters, and patch antennas [54]–[60]. Patch resonators exhibit a number of attractive features, the most important of which are geometrical simplicity and straightforward design process as compared to other structures [37]. So far, patch resonators have been only sparsely used in the design of power dividers. In this work, we demonstrate that patch resonators and patch filters can be useful in design of compact and filtering power dividers. In particular, we propose a divider operating at 1.8 GHz, and implemented using two-patch LPFs featuring simple structure, and three open stubs at each port. The LPFs provide wide stopband with low insertion loss. The wide stopband enables suppression of the unwanted harmonics of the divider. Additional harmonics suppression is achieved by the aforementioned open stubs at each port. The major technical contribution of this work include the development of a filtering H-shaped patch power divider featuring simple structure and harmonic suppression ability. The design exhibiting similar properties has not been demonstrated in the literature before. Furthermore, it is shown that the H-shaped patch resonator along with the open-ended stubs at each port can be used in the Wilkinson power

divider, which results in performance improvement of the device. Comprehensive comparison of the proposed design with the state of the art power dividers demonstrates superior performance of the proposed device. The proposed divider is validated numerically and experimentally, and favorably benchmarked against the state-of-the-art circuits reported in the literature.

## II. DESIGN PROCEDURE OF THE PROPOSED WPD

A conventional Wilkinson power divider (WPD) contains two main branches with the lengths of a quadrature wavelength, and a lumped 100-ohm resistor between the two output ports. This structure is affected by the presence of unwanted harmonics in the frequency response. To overcome this drawback, an alternative structure of a divider is proposed, which will be discussed in the next sections. The conceptual illustration of the design procedure of the proposed WPD has been shown in Fig. 1. Step 1 depicts the key idea of the divider, which incorporates the filtering property of the low pass filters (LPFs) while retaining the overall structure of the conventional WPD. To design the circuit, a new LPF is proposed, as illustrated in Step 2 (a basic LPF) and Step 3 (two high impedance open-ended stubs added to the basic filter). In Step 4, the designed filters are inserted into the main branches of the conventional WPD. Subsequently, based on the major idea of the proposed circuit, three open ended stubs are added at each port to arrive at the final architecture, as shown in Step 5. Step 6 demonstrates the photograph of the fabricated divider prototype.

## III. PROPOSED PATCH LPF

As elaborated on in Section II, one of the main components of the proposed divider is a patch LPF. It is designed to suppress at least the second and the third harmonics. To develop the filters, the basic LPF is first obtained, followed by the final filter architecture.

### A. BASIC LPF CIRCUIT MODEL

The circuit model of the presented basic lowpass filter includes three shunted branches of series LC resonators as suppressors, along with two inductors as the main signal path, which is shown in Fig. 2(a). The S-parameters of the circuit model are shown in Fig. 2(b). The series LC resonators consisting of $l_3C_1$ and $l_2C_2$ create two transmission zeros denoted as $TZ_1$, and $TZ_2$, respectively, which are indicated in Fig. 1(b). The frequency locations of these zeros can be adjusted by tuning the lumped elements values, based on the following equations

$$\text{Frequency of } TZ_1 = \frac{1}{2\pi\sqrt{l_3C_1}} \tag{1}$$

$$\text{Frequency of } TZ_2 = \frac{1}{2\pi\sqrt{l_2C_2}} \tag{2}$$

By adjusting the locations of the transmission zeros, the desired passband and the suppression band for the basic filter can be obtained. Subsequently, the equivalent transmission

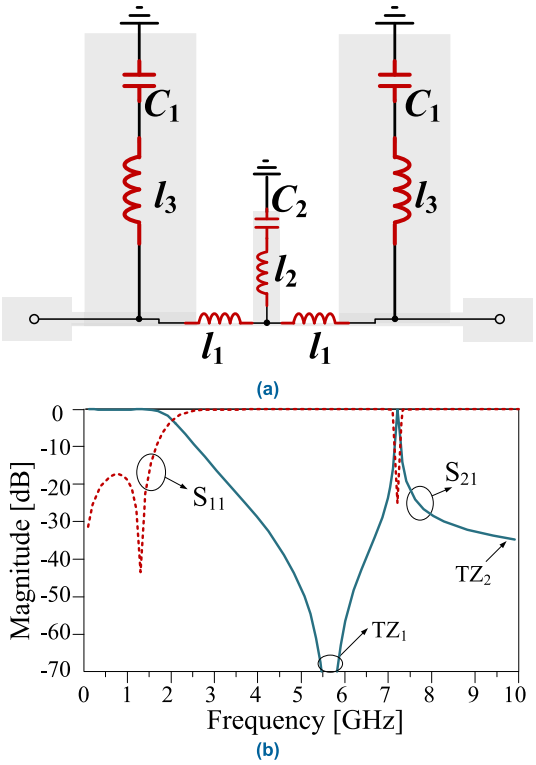


**FIGURE 2.** Circuit model of the presented basic LPF: (a) schematic diagram, (b) simulated S-parameters; $|S_{21}|$ and $|S_{11}|$ are shown using solid and dashed lines, respectively. Parameters of $TZ_1$ and $TZ_2$ show the locations of the first and second transmission zeros created by the LC resonators. $TZ_2$ is located at higher frequencies near 18 GHz.

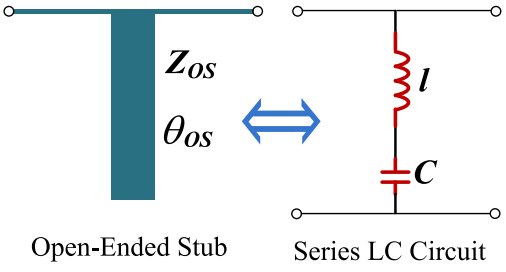


**FIGURE 3.** The equivalent network model of the open-ended stub for the shunted branch of the series LC resonator. The electrical length and the impedance of the open-ended stub are indicated as $\theta_{OS}$ and $Z_{OS}$, respectively.

line dimensions can be calculated using the relations.

$$\text{ABCD}_{LC} = \begin{bmatrix} 1 & 0 \\ \dfrac{1}{jL\omega + \dfrac{1}{jC\omega}} & 1 \end{bmatrix} \tag{3}$$

$$\text{ABCD}_{OS} = \begin{bmatrix} 1 & 0 \\ j\dfrac{\tan(\theta_{OS})}{Z_{OS}} & 1 \end{bmatrix} \tag{4}$$

that provide the ABCD matrices of a series LC resonator and the open-ended stub (eqns. (3) and (4)), shown in Fig. 3. Equivalent dimensions of the open-ended stub can be found

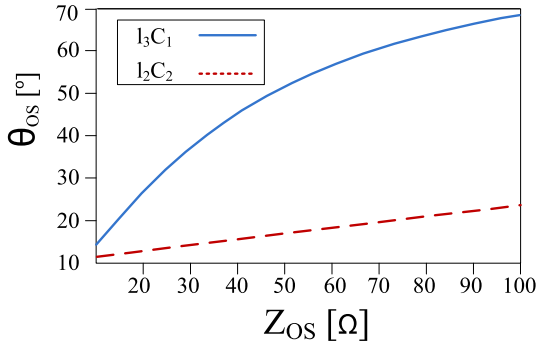


**FIGURE 4.** Calculated dimensions of the equivalent open-ended stub for the $l_3$ $C_1$ and $l_2$ $C_2$ resonators. The electrical length and the impedance of the open-ended stub are indicated as $\theta_{OS}$ and $Z_{OS}$, respectively. In this figure, the lumped element values of $l_3$, $C_1$, $l_2$, and $C_2$ are considered based on values in Table 1.

by comparing (3) and (4), which leads to

$$\theta_{OS} = \tan^{-1}\left(\frac{Z_{OS}C\omega}{1 - LC\omega^2}\right) \tag{5}$$

representing the electrical length of the equivalent open-ended stub. Equation (5) is solved for a typical open-ended stub transmission line. The calculated dimensions of the equivalent open-ended stub for the $l_3C_1$ and $l_2C_2$ resonators are shown in Fig. 4.

Figure 5 illustrates the flowchart of the design procedure of the proposed divider. The figure also indicated how to utilize the extracted equations to design the resonators, patch

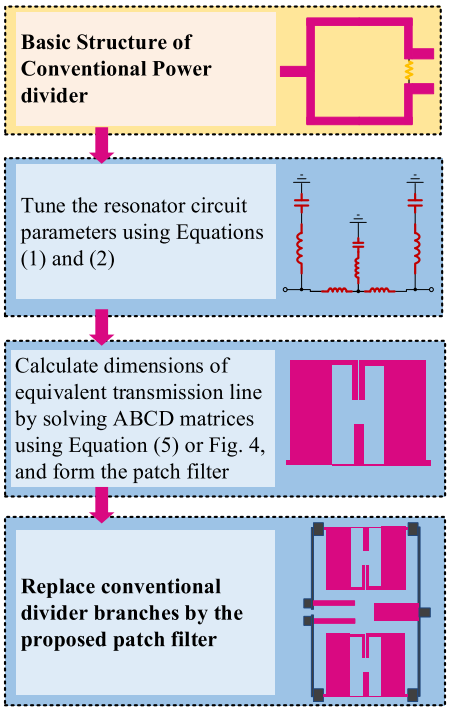


**FIGURE 5.** Flowchart of the design procedure of the proposed divider. In the figure, instructions of using equations for designing the final patch power divider is explained in different steps.

**TABLE 1.** The values of lumped elements and equivalent transmission line dimensions of the basic filter circuit model.

| Element | Value | Element | Value |
|---|---|---|---|
| $l_1$ (nH) | 3.2 | $\theta_{os1}$ (degree) | 32 |
| $l_2$ (nH) | 0.3 | $\theta_{os2}$ (degree) | 11 |
| $l_3$ (nH) | 0.4 | $Z_{os1}$ (ohm) | 25 |
| $C_1$ (pF) | 2 | $Z_{os2}$ (ohm) | 66 |
| $C_2$ (pF) | 0.25 | | |

The parameters of $\theta_{os1}$, $Z_{os1}$ and $\theta_{os2}$, $Z_{os2}$ are equivalent open-ended stub dimensions corresponding to $l_3C_1$ and $l_2C_2$ resonators, respectively.

filter and the patch power divider. The values of the lumped elements and the equivalent transmission line dimensions of the basic filter circuit model, obtained using the above analysis, are listed in Table 1.

After calculating the transmission line dimensions of the basic LPF, it can be realized using microstrip transmission lines, which is described in the next subsection.

### B. BASIC LPF DESIGN

The basic filter is implemented using the high impedance line of a 0.1-mm width inserted between the ports, loaded by two low impedance capacitive open-ended stubs on both sides of the filter, along with a smaller single open-ended stub in the middle of the filter. Figure 6 demonstrates the

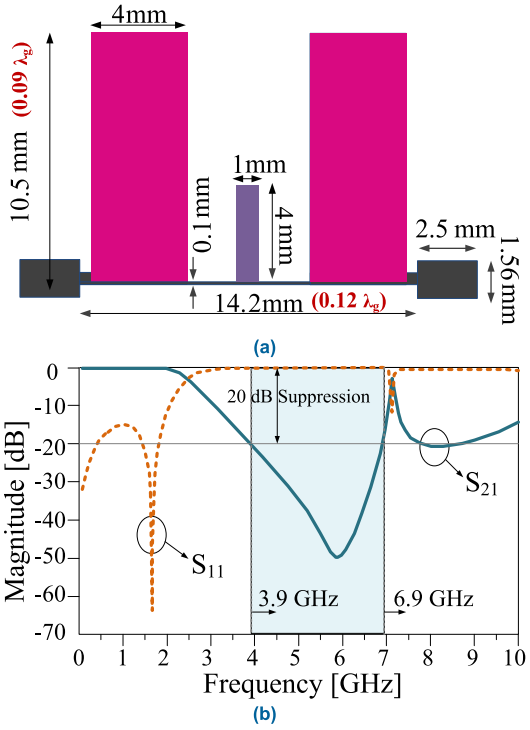


**FIGURE 6.** Basic structure of the proposed LPF: (a) layout, (b) simulated S-parameters; $|S_{21}|$ and $|S_{11}|$ are shown using solid and dashed lines, respectively. The highlighted square between 3.9 GHz and 6.9 GHz shows the suppression band with 20 dB attenuation level.

layout and simulated S-parameters of the proposed basic LPF, implemented on the Rogers RT5880 substrate. The circuit dimensions are provided in Fig. 6(a). It should be observed that the basic LPF frequency response is not sharp enough. The filter exhibits a 3 GHz suppression band from 3900 MHz to 6900 MHz with 20 dB attenuation.

### C. PROPOSED PATCH LPF

As mentioned, the basic LPF does not have a sufficiently sharp response, and features a limited stopband, which fails to suppress the second harmonic in the final power divider at 3.6 GHz. To improve the filter performance, the structure is enhanced by adding two high impedance open-ended stubs as shown in Fig. 7(a). The simulated frequency response of the proposed patch LPF is demonstrated in Fig. 7(b). A sharp transmission response can be observed as well as the enhanced stopband of 3200 MHz to 6500 MHz with 20 dB attenuation. The cutoff frequency of the patch LPF is 2.2 GHz. This is suitable for designing the 1.8 GHz power divider, as the location of the cutoff frequency of the LPF should be higher than the desired operating frequency of the power divider. At the same time, the cutoff frequency of the LPF should be lower than the frequency of the second harmonic to enable suppression of the latter. Both conditions are met by the proposed LPF structure.

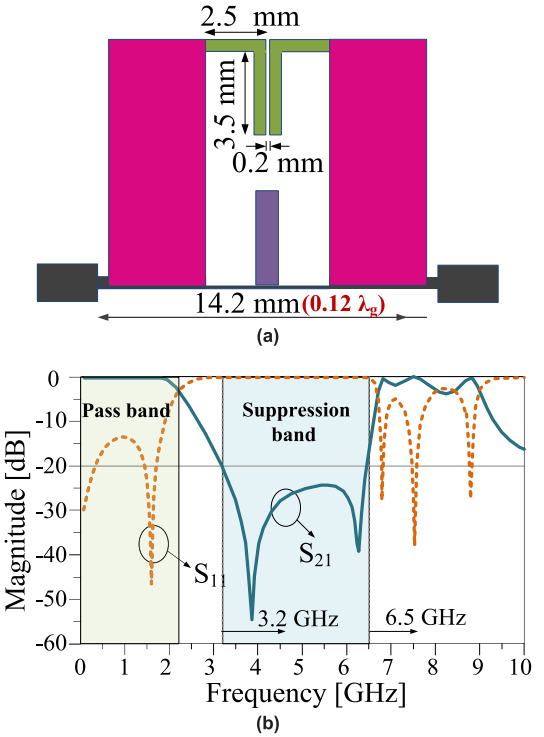


**FIGURE 7.** Final structure of the proposed LPF: (a) layout, (b) simulated S-parameters; $|S_{21}|$ and $|S_{11}|$ are shown using solid and dashed lines, respectively. The right-hand-side highlighted square between 3.2 GHz and 6.9 GHz shows the suppression band with 20 dB attenuation level. The left-hand-side highlighted square from 0 GHz to 2.2 GHz represent the passband of the filter.

## IV. PROPOSED PATCH POWER DIVIDER

As explained in Section III, by utilizing the LPFs presented therein, the entire structure of the designed WPD can be developed. At first, the LPFs LC models are added to the divider circuit model. The final LC model and its frequency response for the proposed patch power divider is depicted in Fig. 8. Also, the values of lumped elements of the proposed patch divider LC model are listed in Table 2. In the following subsections, the transmission line realization of the proposed divider circuit model is studied.

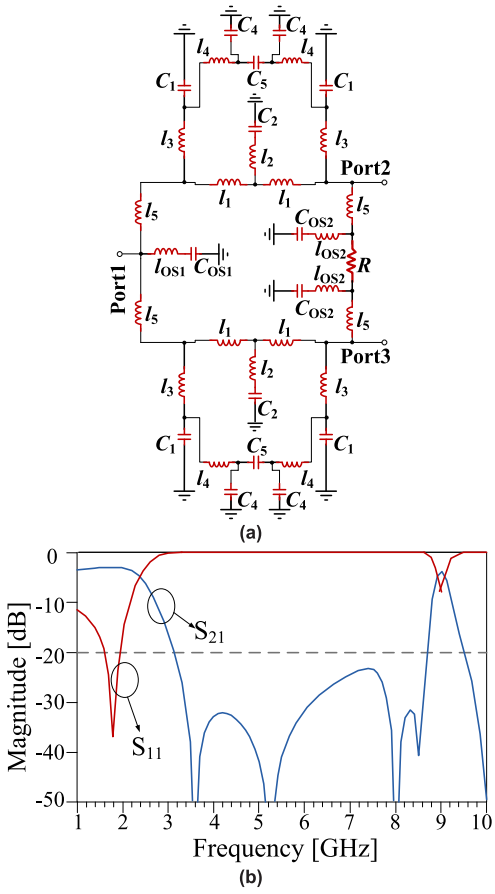


**FIGURE 8.** (a) The final LC model and its (b) frequency response for the proposed patch power divider.

**TABLE 2.** The values of lumped elements of the proposed patch divider LC model.

| Element | Value | Element | Value |
|---|---|---|---|
| $l_1$ (nH) | 3 | $C_1$ (pF) | 0.7 |
| $l_2$ (nH) | 0.8 | $C_2$ (pF) | 0.05 |
| $l_3$ (nH) | 1.2 | $C_4$ (pF) | 0.3 |
| $l_4$ (nH) | 1.6 | $C_5$ (pF) | 0.02 |
| $l_5$ (nH) | 0.6 | $C_{OS1}$ (pF) | 0.01 |
| $l_{OS1}$ (nH) | 10 | $C_{OS2}$ (pF) | 0.05 |
| $l_{OS2}$ (nH) | 8 | | |

### A. BASIC PATCH POWER DIVIDER

By replacing the conventional WPD branches with the new LPFs, the structure of the basic patch power divider is formed, which is illustrated in Fig. 9. The overall size of WPD is 29.9 mm × 18.3 mm (0.25 λ × 0.15 λ). Figure 9 demonstrates the layout and the simulated S-parameters of the designed basic patch power divider. The basic divider structure works at the operating band of 1.8 GHz to 2 GHz. As depicted in Fig. 9, the isolation and return loss do not reach acceptable levels in the operating band, whereas the suppression band is not sufficiently broad. Both need further improvements, which is described in the next subsection.

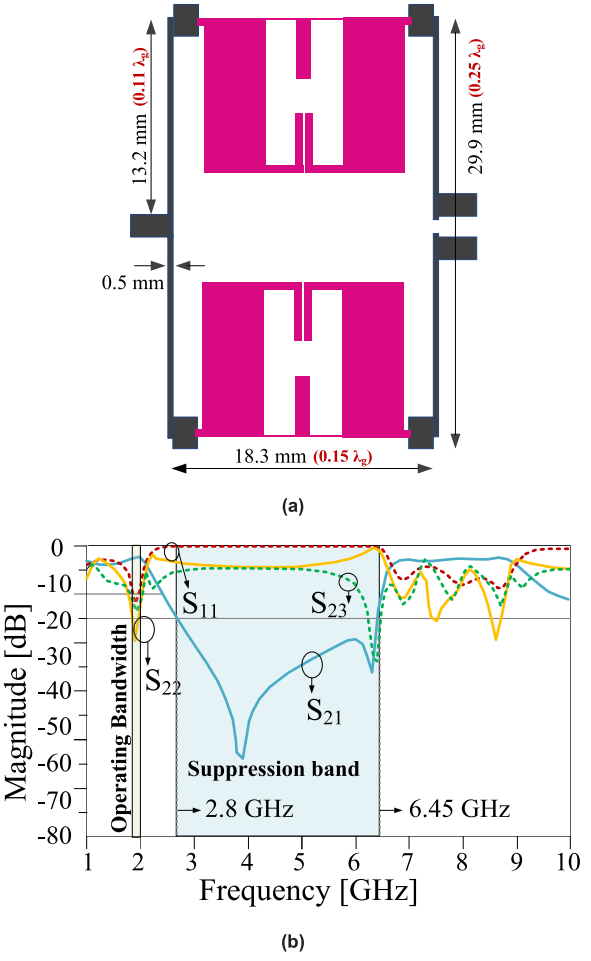


**FIGURE 9.** Structure of the basic patch power LPF: (a) layout, (b) simulated S-parameters; $|S_{21}|$ and $|S_{22}|$ are shown using solid lines, whereas $|S_{23}|$ and $|S_{11}|$ are shown using the dashed lines. The right-hand-side highlighted square between 2.8 GHz and 6.45 GHz shows the suppression band with 20 dB attenuation level. The left-hand-side highlighted square from 1.8 GHz to 2 GHz represent the operating bandwidth of the basic patch power divider, considering 10 dB attenuation level.

### B. PROPOSED PATCH POWER DIVIDER

By adding three open stubs at each port of the basic patch power divider, intended to improve the operating bandwidth and the suppression band, the final architecture is constructed. Figure 10 shows the layout of the proposed patch power divider. Adding three open stubs does not change the overall size of the divider, which is still 0.24 λ × 0.15 λ. The current distributions of the proposed divider at different frequencies are depicted in Fig. 11. As it can be seen, the high-magnitude current is conducted by the divider at the main frequency, while it is reduced at harmonics frequencies.

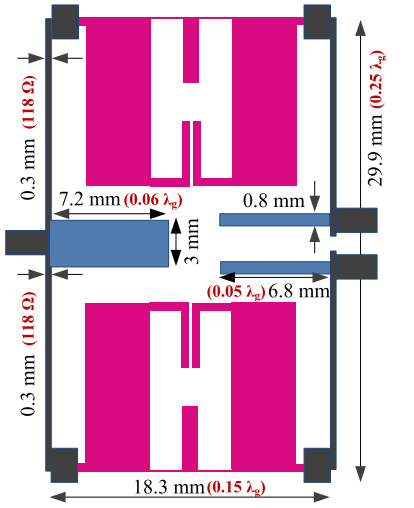


**FIGURE 10.** The structure of the proposed patch divider. Three open ended stubs, added in the divider structure, are shown with different color in the layout.

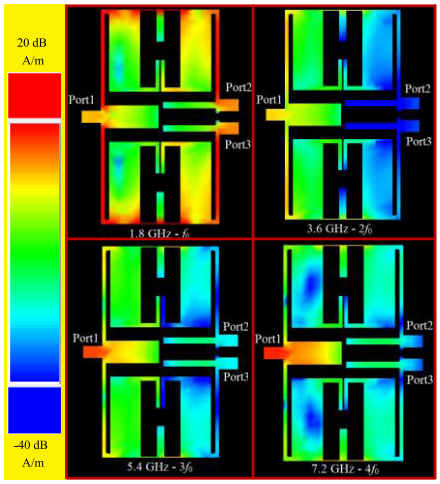


**FIGURE 11.** The current distributions of the proposed divider at different frequencies. the main frequency ($f_0$), second harmonic frequency ($2f_0$), third harmonic frequency ($3f_0$), and fourth harmonic frequency ($4f_0$) are considered in this figure.

## V. EVEN- AND ODD-MODE ANALYSES OF THE PROPOSED PATCH POWER DIVIDER

In this Section, even- and odd-mode circuits of the proposed divider are extracted, as shown in Fig. 12, and the divider is analyzed based on these circuits.

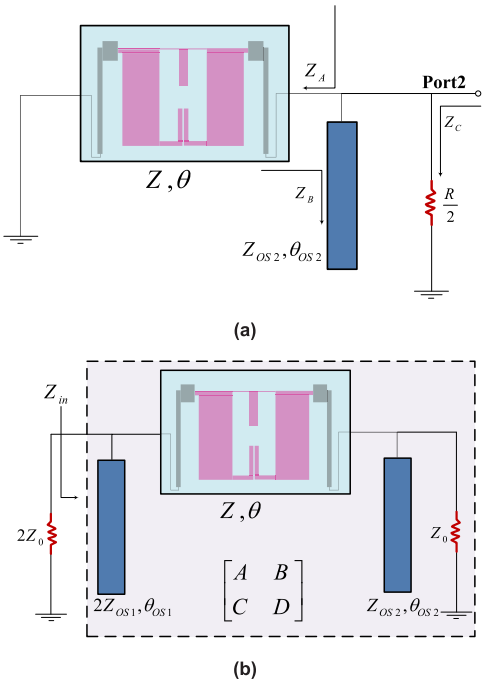


**FIGURE 12.** (a) The odd-mode equivalent circuit of the proposed divider. To extract the odd mode circuit of the divider, a short circuit line is placed along plane of symmetry. (b) The even-mode equivalent circuit of the proposed divider. To extract the even mode circuit of the divider, an open circuit line is placed along plane of symmetry. The square with dashed line in the figure indicates the area, in which the ABCD matrix is provided.

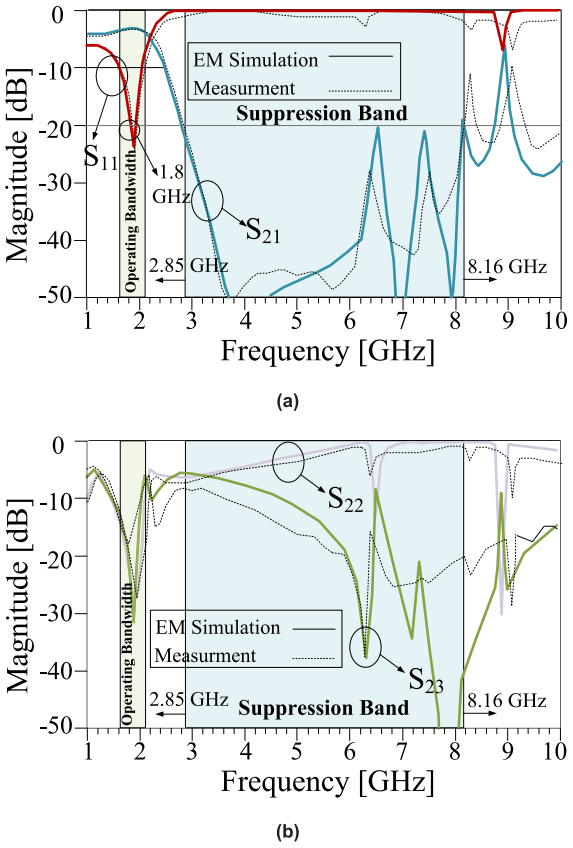


**FIGURE 13.** Verification of the proposed divider circuit: (a) simulated (–) and measured (· · · ·) $|S_{21}|$, $|S_{11}|$, (b) $|S_{22}|$, and $|S_{23}|$ parameters. The right-hand-side highlighted square between 2.85 GHz and 8.16 GHz shows the suppression band with 20 dB attenuation level. The left-hand-side highlighted square from 1.62 GHz to 2.1 GHz represent the operating bandwidth of the proposed patch power divider, considering 10 dB attenuation level.

### A. ODD-MODE ANALYSIS

The odd-mode equivalent circuit of the proposed divider, extracted for odd-mode analysis has been shown in Fig. 12(a). To extract the odd-mode circuit of the divider, a short circuit line is placed along the plane of symmetry. The proposed LPF is equated by a single transmission line with $Z_{LPF}$ and $\theta_{LPF}$ dimensions. Also, $Z_{OS2}$ and $\theta_{OS2}$ corresponds to the open-ended stub, connected to Port2. Equation (6) shows that the overall impedances seen from Port2 should match $Z_0 = 50\ \Omega$ or the normalized value of $Z_0 = 1$.

$$1 = \frac{1}{Z_A} + \frac{1}{Z_B} + \frac{1}{Z_C} \tag{6}$$

By substitution the corresponding values of $Z_A$, $Z_B$, and $Z_C$, (6) can be written as

$$1 = \frac{-j}{Z_{LPF} \tan\theta_{LPF}} + \frac{j \tan\theta_{OS2}}{Z_{OS2}} + \frac{2}{R} \tag{7}$$

Equating the real parts of both sides of (7) yields normalized $R = 2$ (Resistor $= 100\ \Omega$), whereas equating the imaginary parts results in (8).

$$Z_{LPF} \tan\theta_{LPF} = \frac{Z_{OS2}}{\tan\theta_{OS2}} \tag{8}$$

### B. EVEN-MODE ANALYSIS

The even-mode equivalent circuit of the proposed divider is depicted in Fig. 12(b). Also, in this figure, the proposed LPF is represented by a single transmission line with $Z_{LPF}$ and $\theta_{LPF}$ dimensions. Subsequently, the even-mode circuit is analyzed by providing the ABCD matrix, which yields to (9).

$$\begin{bmatrix} A & B \\ C & D \end{bmatrix} = \begin{bmatrix} 1 & 0 \\ \frac{j \tan\theta_{OS1}}{2Z_{OS1}} & 1 \end{bmatrix} \times \begin{bmatrix} \cos\theta_{LPF} & jZ_{LPF} \sin\theta_{LPF} \\ \frac{j \sin\theta_{LPF}}{Z_{LPF}} & \cos\theta_{LPF} \end{bmatrix} \times \begin{bmatrix} 1 & 0 \\ \frac{j \tan\theta_{OS2}}{Z_{OS2}} & 1 \end{bmatrix} \times \begin{bmatrix} 1 & 0 \\ 1 & 1 \end{bmatrix} \tag{9}$$

As it can be concluded from the even-mode circuit, the total impedance, seen from Port1, should be equal to $2Z_0$, or the normalized value of 2 (100 Ω). By solving (9) and equating input impedance, extracted from ABCD matrix, to the normalized value of 2, the following relationships can be obtained

$$Z_{LPF} \sin\theta_{LPF} = \sqrt{2} \tag{10}$$

$$Z_{LPF} \tan\theta_{LPF} = \frac{2Z_{OS1}}{\tan\theta_{OS1}} \tag{11}$$

In practice, to facilitate the design procedure of the proposed divider, the length of the open-ended stubs can be

**TABLE 3. Comparison between the performances of the proposed patch power divider and related state of the arts dividers.**

| Ref. | Freq. (GHz) | IL (dB) | HS | Size ($\lambda_g \times \lambda_g$) | MTHD | Type |
|---|---|---|---|---|---|---|
| [21] | 1 | 1.1 | 2nd & 3rd | 0.50 × 0.58 | - Open Stub | GPD |
| [61] | 1 | 0.8 | 2nd | 0.29 × 0.34 | - Coupled Lines<br>- Open Stubs | WPD |
| [62] | 2 | 0.7 | 2nd | 0.33 × 0.25 | - Coupled Lines<br>- Open Stubs | FPD |
| [63] | 1 | 0.2 | 2nd to 5th | 0.43 × 0.34 | - Coupled Lines<br>- Lumped Elements | FPD |
| [64] | 3 | 0.6 | 2nd | 0.52× 0.29 | - Coupled Lines<br>- Lumped Elements | FPD |
| [65] | 1 | 0.45 | 2nd to 5th | 0.20 × 0.40 | - SIR | BTUPD |
| **This work** | 1.8 | 0.5 | 2nd to 11th | 0.25 × 0.15 | - Patch Resonators<br>- Open Stubs | WPD |

The meaning of abbreviations utilized in the table:
- Ref. – reference,
- Freq. – operating frequency,
- IL – insertion loss,
- HS – harmonic suppression,
- MTHD – method (i.e., major circuit solutions utilized in the considered structure),
- GPD – Gysel power divider,
- WPD – Wilkinson power divider,
- FPD – filtering power divider,
- SIR – stepped impedance resonators,
- BTUPD – balanced to unbalanced power divider.

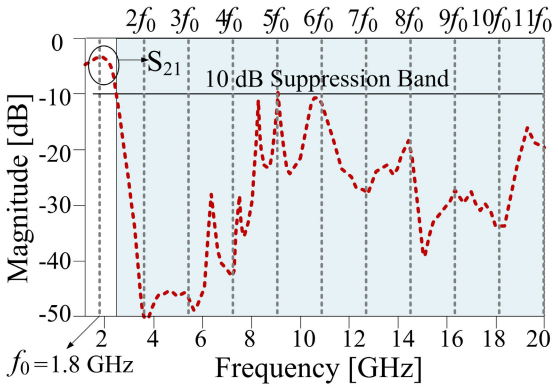


**FIGURE 14. The frequency response of the designed patch power divider in a wide range frequency. The highlighted square between 2.5 GHz and 20 GHz shows the suppression band with 10 dB attenuation level.**

considered equal, so by using (8) and (11), the relation between impedances of the open-ended stubs will be obtained as

$$Z_{OS2} = 2Z_{OS1} \tag{12}$$

The lengths of the open-stubs should be adjusted in order to allocate the transmission zeros at the frequencies ensuring the best possible suppression band. Therefore, the lengths of the open-stubs are considered equal as $\theta = 20°$, and, subsequently the values of $Z_{OS1} = 30\ \Omega$ and $Z_{OS2} = 60\ \Omega$ are selected based on (12) and size limitation of the power divider structure. Finally, based on (10) and (11), the overall values of equivalent transmission line for the LPF along with its lateral branches will be achieved as $Z_{LPF} = 78.3\ \Omega$, $\theta_{LPF} = 64.6°$.

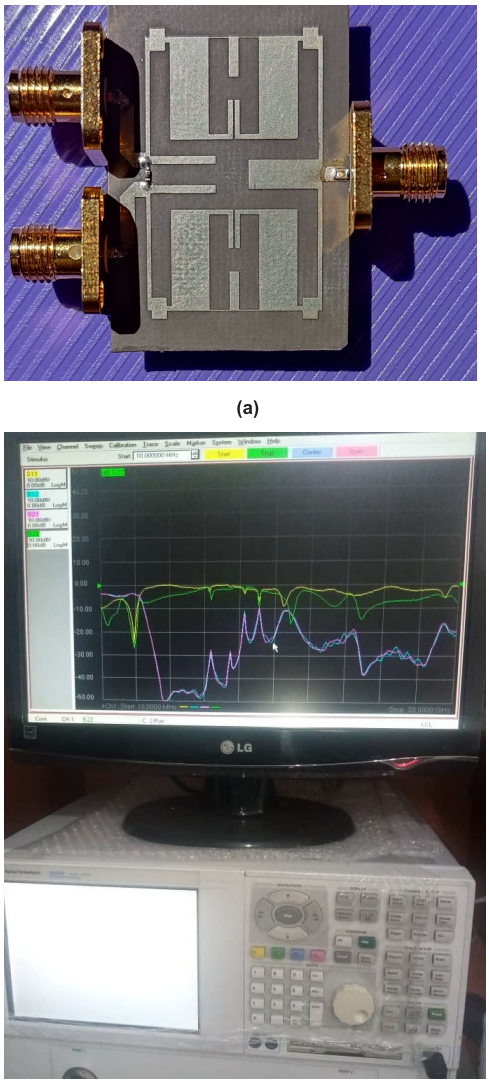


**FIGURE 15. Photographs of the fabricated prototype of the proposed divider circuit (a), and the measurement setup (b).**

## VI. FABRICATION AND MEASUREMENT RESULTS

The proposed patch divider has been fabricated on the Rogers RT5880 substrate. Figure 13 demonstrates the simulated and measured S-parameters of the designed patch power divider circuit. According to the results, the divider correctly works at the main frequency of 1.8 GHz. The operating bandwidth is 480 MHz, from 1620 MHz to 2100 MHz, which corresponds to a relative bandwidth of 25.8 percent. Furthermore, the measured results indicate that $|S_{11}|$, $|S_{12}|$, $|S_{13}|$, $|S_{22}|$, and $|S_{23}|$, are −17 dB, −3.5 dB, −3.33 dB, −20 dB, and −17 dB, respectively, all at the operating frequency. Also, a suppression band of more than 5 GHz is obtained from 2850 MHz to 8160 MHz, showing 2nd to 4th harmonic suppression, considering 20 dB attenuation level. In order to provide a better clarification of the harmonic suppression ability of the divider, the overall frequency response of the proposed patch power divider is illustrated in Figure 14, showing 2nd to 11th harmonic suppression, considering 10 dB attenuation level.

The photographs of the fabricated prototype of the proposed divider circuit and the measurement setup are depicted in Fig. 15. The measurement of the circuit S-parameters has been carried out using the Agilent E8362B Network Analyzer. Table 2 shows a performance comparison between the designed patch WPD and the state-of-the-art circuits from the literature. Although the proposed structure is geometrically simple, its performance is superior over the benchmark, including power dividers that are much more topologically involved. This is also pertinent to the harmonic suppression capability, which is unmatched by the structured included in the comparison set.

## VII. CONCLUSION

In this paper, a simple patch power divider with ultra-wideband harmonics suppression band has been proposed. For the first time, a simple H-shaped patch filter has been incorporated into the divider structure along with additional open-ended stubs, which results in extremely wide range of frequency rejection, up to the eleventh harmonic. A detailed design procedure has been provided to facilitate the parameter adjustment. Full-wave EM simulations and physical measurements of the fabricated divider prototype corroborate the efficacy of the proposed circuit solution. Moreover, the performance of the presented divider has been favorably compared to the related state-of-the-art dividers, showing the advantages of the proposed work, which include considerably better harmonic suppression capability while maintaining topological simplicity of the circuit.

## REFERENCES

[1] M. B. Jamshidi, S. Roshani, J. Talla, S. Roshani, and Z. Peroutka, "Size reduction and performance improvement of a microstrip Wilkinson power divider using a hybrid design technique," *Sci. Rep.*, vol. 11, no. 1, pp. 1–15, Dec. 2021.

[2] C.-M. Lin, H.-H. Su, J.-C. Chiu, and Y.-H. Wang, "Wilkinson power divider using microstrip EBG cells for the suppression of harmonics," *IEEE Microw. Wireless Compon. Lett.*, vol. 17, no. 10, pp. 700–702, Oct. 2007.

[3] L. Yang, M. Fan, F. Chen, J. She, and Z. Feng, "A novel compact electromagnetic-bandgap (EBG) structure and its applications for microwave circuits," *IEEE Trans. Microw. Theory Techn.*, vol. 53, no. 1, pp. 183–190, Jan. 2005.

[4] P. P. Bhavarthe, S. S. Rathod, and K. T. V. Reddy, "A compact dual band gap electromagnetic band gap structure," *IEEE Trans. Antennas Propag.*, vol. 67, no. 1, pp. 596–600, Jan. 2019.

[5] B. P. Smyth and A. K. Iyer, "Dual-band Wilkinson power divider using uniplanar metamaterial-based EBGs," in *Proc. IEEE Int. Symp. Antennas Propag. USNC/URSI Nat. Radio Sci. Meeting*, Jul. 2017, p. 457.

[6] J. Selga, P. Vélez, J. Bonache, and F. Martín, "EBG-based transmission lines with slow-wave characteristics and application to miniaturization of microwave components," *Appl. Phys. A, Solids Surf.*, vol. 123, no. 1, pp. 1–6, Jan. 2017.

[7] C. Han, D. Tang, Z. Deng, H. J. Qian, and X. Luo, "Filtering power divider with ultrawide stopband and wideband low radiation loss using substrate integrated defected ground structure," *IEEE Microw. Wireless Compon. Lett.*, vol. 31, no. 2, pp. 113–116, Feb. 2021.

[8] L. H. Weng, Y.-C. Guo, X.-W. Shi, and X.-Q. Chen, "An overview on defected ground structure," *Prog. Electromagn. Res. B*, vol. 7, pp. 173–189, 2008.

[9] H. Oraizi and M. S. Esfahlan, "Miniaturization of Wilkinson power dividers by using defected ground structures," *Prog. Electromagn. Res. Lett.*, vol. 4, pp. 113–120, 2008.

[10] M. Salman, Y. Jang, J. Lim, D. Ahn, and S.-M. Han, "Novel Wilkinson power divider with an isolation resistor on a defected ground structure with improved isolation," *Appl. Sci.*, vol. 11, no. 9, p. 4148, May 2021.

[11] M. K. Hedayati, G. Moradi, and A. Abdipour, "Improved dual-frequency Wilkinson power dividers with defected ground structure," *IEICE Electron. Exp.*, vol. 8, no. 11, pp. 808–813, 2011.

[12] Z. He, J. Cai, Z. Shao, X. Li, and Y. Huang, "A novel power divider integrated with SIW and DGS technology," *Prog. Electromagn. Res.*, vol. 139, pp. 289–301, 2013.

[13] Y. Wu, Y. Liu, and S. Li, "Unequal dual-frequency Wilkinson power divider including series resistor-inductor-capacitor isolation structure," *IET Microw., Antenna Propag.*, vol. 3, no. 7, pp. 1079–1085, Jul. 2009.

[14] P. Rostami and S. Roshani, "A miniaturized dual band Wilkinson power divider using capacitor loaded transmission lines," *AEU-Int. J. Electron. Commun.*, vol. 90, pp. 63–68, Jun. 2018.

[15] Y. Lu, G. Dai, Y. Wang, T. Liu, and J. Huang, "Dual-band filtering power divider with capacitor-loaded centrally coupled-line resonators," *IET Microw., Antennas Propag.*, vol. 11, no. 1, pp. 36–41, 2017.

[16] B. Xia, J.-D. Cheng, L.-S. Wu, C. Xiong, and J.-F. Mao, "A new compact power divider based on capacitor central loaded coupled microstrip line," *IEEE Trans. Microw. Theory Techn.*, vol. 68, no. 10, pp. 4249–4256, Oct. 2020.

[17] J.-L. Li, H.-Z. Wang, J.-P. Wang, S.-S. Gao, X.-S. Yang, and W. Shao, "Miniaturized Wilkinson power dividers with harmonic suppressions," *Electromagnetics*, vol. 36, no. 3, pp. 157–166, Apr. 2016.

[18] R. Mirzavand, M. M. Honari, A. Abdipour, and G. Moradi, "Compact microstrip Wilkinson power dividers with harmonic suppression and arbitrary power division ratios," *IEEE Trans. Microw. Theory Techn.*, vol. 61, no. 1, pp. 61–68, Jan. 2013.

[19] Y.-C. Yoon and Y. Kim, "Miniaturized multi-section power divider with parallel RC isolation circuit," *J. Electromagn. Eng. Sci.*, vol. 19, no. 3, pp. 147–152, Jul. 2019.

[20] S. Roshani and S. Roshani, "Design of a compact LPF and a miniaturized Wilkinson power divider using aperiodic stubs with harmonic suppression for wireless applications," *Wireless Netw.*, vol. 26, no. 2, pp. 1493–1501, Feb. 2020.

[21] E. Moradi, A.-R. Moznebi, K. Afrooz, and M. Movahhedi, "Gysel power divider with efficient second and third harmonic suppression using one resistor," *AEU-Int. J. Electron. Commun.*, vol. 89, pp. 116–122, May 2018.

[22] K. D. Xu, J. Xu, and D. Li, "Wilkinson filtering power divider using coupled lines and T-shaped stub," *Microw. Opt. Technol. Lett.*, vol. 61, no. 11, pp. 2540–2544, 2019.

[23] Z. He, K. Song, B. Zeng, Y. Zhu, and Y. Fan, "Miniaturized tri-band filtering-response power divider with short-and open-stub-loaded resonators," *Int. J. Microw. Wireless Technol.*, vol. 9, no. 8, pp. 1637–1643, 2017.

[24] F.-X. Liu, Y. Wang, X.-Y. Zhang, C.-H. Quan, and J.-C. Lee, "A size-reduced tri-band Gysel power divider with ultra-wideband harmonics suppression performance," *IEEE Access*, vol. 6, pp. 34198–34205, 2018.

[25] H. Jaradat, N. Dib, and K. Al Shamaileh, "Miniaturized dual-band CPW Wilkinson power divider using T-network adopting series stubs with a high frequency ratio," *AEU-Int. J. Electron. Commun.*, vol. 107, pp. 32–38, Jul. 2019.

[26] A. Sahu, K. A. Al Shamaileh, P. H. Aaen, S. A. Abushamleh, and V. K. Devabhaktuni, "A high-frequency/power ratio Wilkinson power divider based on identical/non-identical multi-T-sections with short-circuited stubs," *IEEE Open J. Circuits Syst.*, vol. 2, pp. 34–45, 2021.

[27] B. Li, X. Wu, N. Yang, and W. Wu, "Dual-band equal/unequal Wilkinson power dividers based on coupled-line section with short-circuited stub," *Prog. Electromagn. Res.*, vol. 111, pp. 163–178, 2011.

[28] C. J. Chen, "A coupled-line isolation network for the design of filtering power dividers with improved isolation," *IEEE Trans. Compon., Packag., Manuf. Technol.*, vol. 8, no. 10, pp. 1830–1837, Oct. 2018.

[29] C.-J. Chen and Z.-C. Ho, "Design equations for a coupled-line type filtering power divider," *IEEE Microw. Wireless Compon. Lett.*, vol. 27, no. 3, pp. 257–259, Mar. 2017.

[30] X. Yu, S. Sun, and Y. Liu, "Design of wideband filtering power dividers with harmonic suppression based on the parallel-coupled line structures," *Appl. Comput. Electromagn. Soc. J.*, vol. 33, no. 5, pp. 468–475, 2018.

[31] M. H. Maktoomi, D. Banerjee, and M. S. Hashmi, "An enhanced frequency-ratio coupled-line dual-frequency Wilkinson power divider," *IEEE Trans. Circuits Syst. II, Exp. Briefs*, vol. 65, no. 7, pp. 888–892, Jul. 2018.

[32] Y.-S. Lin and K.-S. Lan, "Spiral-coupled-line-based Wilkinson power divider," *IEEE Microw. Wireless Compon. Lett.*, vol. 31, no. 3, pp. 241–244, Mar. 2021.

[33] M. Jamshidi, H. Siahkamari, S. Roshani, and S. Roshani, "A compact Gysel power divider design using U-shaped and T-shaped resonators with harmonics suppression," *Electromagnetics*, vol. 39, no. 7, pp. 491–504, Oct. 2019.

[34] Q. Li, Y. Zhang, and C.-T. M. Wu, "High-selectivity and miniaturized filtering Wilkinson power dividers integrated with multimode resonators," *IEEE Trans. Compon., Packag., Manuf. Technol.*, vol. 7, no. 12, pp. 1990–1997, Dec. 2017.

[35] H. Zhu, Z. Cheng, and Y. J. Guo, "Design of wideband in-phase and out-of-phase power dividers using microstrip-to-slotline transitions and slotline resonators," *IEEE Trans. Microw. Theory Techn.*, vol. 67, no. 4, pp. 1412–1424, Apr. 2019.

[36] W. Feng, W. Che, Y. Shi, Q. Xue, Y. C. Li, and X. Y. Zhou, "High selectivity balanced-to-unbalanced filtering power dividers using dual-mode ring resonators," *IEEE Trans. Compon., Packag., Manuf. Technol.*, vol. 9, no. 5, pp. 927–935, Aug. 2018.

[37] Q. Liu, J. Wang, L. Zhu, G. Zhang, and W. Wu, "Design of a new balanced-to-balanced filtering power divider based on square patch resonator," *IEEE Trans. Microw. Theory Techn.*, vol. 66, no. 12, pp. 5280–5289, Dec. 2018.

[38] G. Zhang, X. Wang, and J. Yang, "Dual-band microstrip filtering power divider based on one single multimode resonator," *IEEE Microw. Wireless Compon. Lett.*, vol. 28, no. 10, pp. 891–893, Oct. 2018.

[39] M. Luo, X. Xu, X.-H. Tang, and Y.-H. Zhang, "A compact balanced-to-balanced filtering Gysel power divider using $\lambda_g/2$ resonators and short-stub-loaded resonator," *IEEE Microw. Wireless Compon. Lett.*, vol. 27, no. 7, pp. 645–647, Jul. 2017.

[40] K. Xu, J. Shi, W. Zhang, and G. M. Mbongo, "The compact balanced filtering power divider with in-phase or out-of-phase output using H-shape resonators," *IEEE Access*, vol. 6, pp. 38490–38497, 2018.

[41] G. Zhang, Z. Qian, J. Yang, and J.-S. Hong, "Wideband four-way filtering power divider with sharp selectivity and high isolation using coshared multi-mode resonators," *IEEE Microw. Wireless Compon. Lett.*, vol. 29, no. 10, pp. 641–644, Oct. 2019.

[42] Q. Zhang, G. Zhang, Z. Liu, X. Tan, W. Tang, and H. Yang, "A new balanced-to-single-ended in-phase filtering power divider based on circular patch resonator with good isolation and wide stopband," *Int. J. RF Microw. Comput.-Aided Eng.*, vol. 31, no. 10, 2021, Art. no. e22839.

[43] M. Danaeian, A.-R. Moznebi, and K. Afrooz, "Super compact dual-band substrate integrated waveguide filters and filtering power dividers based on evanescent-mode technique," *AEU-Int. J. Electron. Commun.*, vol. 125, Oct. 2020, Art. no. 153348.

[44] M. Roshani, G. T. T. Phan, P. J. M. Ali, G. H. Roshani, R. Hanus, T. Duong, E. Corniani, E. Nazemi, and E. M. Kalmoun, "Evaluation of flow pattern recognition and void fraction measurement in two phase flow independent of oil pipeline's scale layer thickness," *Alexandria Eng. J.*, vol. 60, no. 1, pp. 1955–1966, 2021.

[45] M. Roshani, G. Phan, G. H. Roshani, R. Hanus, B. Nazemi, E. Corniani, and E. Nazemi, "Combination of X-ray tube and GMDH neural network as a nondestructive and potential technique for measuring characteristics of gas–oil–water three phase flows," *Measurement*, vol. 168, Jan. 2021, Art. no. 108427.

[46] M. Amir Sattari, G. Hossein Roshani, R. Hanus, and E. Nazemi, "Applicability of time-domain feature extraction methods and artificial intelligence in two-phase flow meters based on gamma-ray absorption technique," *Measurement*, vol. 168, Jan. 2021, Art. no. 108474.

[47] M. Roshani, G. Phan, R. H. Faraj, N.-H. Phan, G. H. Roshani, B. Nazemi, E. Corniani, and E. Nazemi, "Proposing a gamma radiation based intelligent system for simultaneous analyzing and detecting type and amount of petroleum by-products," *Nucl. Eng. Technol.*, vol. 53, no. 4, pp. 1277–1283, Apr. 2021.

[48] M. Roshani, M. A. Sattari, P. J. Muhammad Ali, G. H. Roshani, B. Nazemi, E. Corniani, and E. Nazemi, "Application of GMDH neural network technique to improve measuring precision of a simplified photon attenuation based two-phase flowmeter," *Flow Meas. Instrum.*, vol. 75, Oct. 2020, Art. no. 101804.

[49] A. Karami, G. Roshani, A. Khazaei, E. Nazemi, and M. Fallahi, "Investigation of different sources in order to optimize the nuclear metering system of gas–oil–water annular flows," *Neural Comput. Appl.*, vol. 32, no. 8, pp. 3619–3631, 2020.

[50] A. Karami, G. H. Roshani, E. Nazemi, and S. Roshani, "Enhancing the performance of a dual-energy gamma ray based three-phase flow meter with the help of grey wolf optimization algorithm," *Flow Meas. Instrum.*, vol. 64, pp. 164–172, Dec. 2018.

[51] G. H. Roshani, R. Hanus, A. Khazaei, M. Zych, E. Nazemi, and V. Mosorov, "Density and velocity determination for single-phase flow based on radiotracer technique and neural networks," *Flow Meas. Instrum.*, vol. 61, pp. 9–14, Jun. 2018.

[52] M. Jamshidi, A. Lalbakhsh, S. Lotfi, H. Siahkamari, B. Mohamadzade, and J. Jalilian, "A neuro-based approach to designing a Wilkinson power divider," *Int. J. RF Microw. Comput.-Aided Eng.*, vol. 30, no. 3, 2020, Art. no. e22091.

[53] S. Roshani, M. B. Jamshidi, F. Mohebi, and S. Roshani, "Design and modeling of a compact power divider with squared resonators using artificial intelligence," *Wireless Pers. Commun.*, vol. 117, no. 3, pp. 2085–2096, Apr. 2021.

[54] L. Leifsson, X. Du, and S. Koziel, "Efficient yield estimation of multiband patch antennas by polynomial chaos-based Kriging," *Int. J. Numer. Model., Electron. Netw., Devices Fields*, vol. 33, no. 6, p. e2722, 2020.

[55] X. Du, L. Leifsson, and S. Koziel, "Rapid multi-band patch antenna yield estimation using polynomial chaos-Kriging," in *Proc. Int. Conf. Comput. Sci.* Springer, 2019, pp. 487–494.

[56] S. Koziel and A. Bekasiewicz, "Inverse and forward surrogate models for expedited design optimization of unequal-power-split patch couplers," *Metrol. Meas. Syst.*, vol. 26, no. 3, pp. 463–473, 2019.

[57] A. Bekasiewicz and S. Koziel, "Novel structure and design of enhanced-bandwidth hybrid quadrature patch coupler," *Microw. Opt. Technol. Lett.*, vol. 60, no. 12, pp. 3073–3076, 2018.

[58] S. Koziel and A. Bekasiewicz, "Multi-objective design optimization of antenna structures using sequential domain patching with automated patch size determination," *Eng. Optim.*, vol. 50, no. 2, pp. 218–234, Feb. 2018.

[59] S. Sun and W. Menzel, "Novel dual-mode balun bandpass filters using single cross-slotted patch resonator," *IEEE Microw. Wireless Compon. Lett.*, vol. 21, no. 8, pp. 415–417, Aug. 2011.

[60] R. Zhang, L. Zhu, and S. Luo, "Dual-mode dual-band bandpass filter using a single slotted circular patch resonator," *IEEE Microw. Wireless Compon. Lett.*, vol. 22, no. 5, pp. 233–235, May 2012.

[61] H. Soleymani and S. Roshani, "Design and implementation of a bandpass Wilkinson power divider with wide bandwidth and harmonic suppression," *Turkish J. Electr. Eng. Comput. Sci.*, vol. 28, no. 1, pp. 414–422, Jan. 2020.

[62] Y. Wang, F. Xiao, Y. Cao, Y. Zhang, and X. Tang, "Novel wideband microstrip filtering power divider using multiple resistors for port isolation," *IEEE Access*, vol. 7, pp. 61868–61873, 2019.

[63] Y. Wu, Z. Zhuang, Y. Liu, L. Deng, and Z. Ghassemlooy, "Wideband filtering power divider with ultra-wideband harmonic suppression and isolation," *IEEE Access*, vol. 4, pp. 6876–6882, 2016.

[64] X. Yu and S. Sun, "A novel wideband filtering power divider with embedding three-line coupled structures," *IEEE Access*, vol. 6, pp. 41280–41290, 2018.

[65] Z. Zhuang, Y. Wu, M. Kong, W. Wang, and Y. Liu, "Dual-band filtering balanced-to-unbalanced impedance-transforming power divider with high frequency ratio and arbitrary power division," *IEEE Access*, vol. 6, pp. 12710–12717, 2018.

**SAEED ROSHANI** (Member, IEEE) received the B.Sc. degree in electrical engineering from Razi University, Kermanshah, Iran, in 2008, the M.Sc. degree in electrical engineering from Shahed University, Tehran, Iran, in 2011, and the Ph.D. degree in electrical engineering from Razi University, in 2015. He is currently an Associate Professor with the Department of Electrical Engineering, Islamic Azad University, Kermanshah. He performed Opportunity Research Program at the Amirkabir University of Technology (Tehran Polytechnics), Iran, from 2014 to 2015. He graduated as the best student of his country among all students of Iran in 2015 and was awarded by the First Vice President and Science, Research and Technology Minister. He has published more than 100 papers in ISI journals and conferences. His research interests include microwave and millimeter-wave devices and circuits and low-power and low-size integrated circuit design.

**SLAWOMIR KOZIEL** (Senior Member, IEEE) received the M.Sc. and Ph.D. degrees in electronic engineering from the Gdansk University of Technology, Poland, in 1995 and 2000, respectively, and the M.Sc. degree in theoretical physics, the M.Sc. degree in mathematics, and the Ph.D. degree in mathematics from the University of Gdansk, Poland, in 2000, 2002, and 2003, respectively. He is currently a Professor with the Department of Engineering, Reykjavik University, Iceland. His research interests include CAD and modeling of microwave and antenna structures, simulation-driven design, surrogate-based optimization, space mapping, circuit theory, analog signal processing, and evolutionary computation and numerical analysis.

**SOBHAN ROSHANI** received the B.Sc. degree in electrical engineering from Razi University, Kermanshah, Iran, in 2010, the M.Sc. degree in electrical engineering from the Iran University of Science and Technology (IUST), Tehran, Iran, in 2012, and the Ph.D. degree in electrical engineering from Razi University, in 2016. He is currently an Assistant Professor with the Department of Electrical Engineering, Kermanshah Branch, Islamic Azad University, Kermanshah. He has published more than 80 papers in international journals and conferences. He is currently the Head of Young Researchers and Elite Club, Islamic Azad University, Kermanshah Branch. His research interests include switching power amplifiers, optimization and neural networks, artificial intelligence, modeling, microwave circuits, power dividers, couplers, filters, and diplexers.

**MOHAMMAD (BEHDAD) JAMSHIDI** (Member, IEEE) received the associate's degree in electronics from the Shamsipour Technical and Vocational College (former American College), Tehran, Iran, in 2005, the B.Sc. degree in telecommunication engineering from the University of Applied Science and Technology, Shiraz, Iran, in 2008, and the M.Sc. degree in mechatronics engineering from Islamic Azad University (IAU), South-Tehran Branch, Tehran, in 2011.

From 2011 to 2019, he was a Senior Researcher with the Young Researchers and Elite Club, IAU. From 2012 to 2017, he was also a full-time Faculty Member with the Department of Electrical Engineering, IAU. He is currently a Researcher with the Research and Innovation Centre for Electrical Engineering, University of West Bohemia, Pilsen, Czech Republic. He has some international collaborations with universities such as the University of California at Berkley; University of Wisconsin–Madison; Waseda University, Tokyo; Seoul National University; Texas A&M University; Louisiana State University; Medical University of Tehran; University of Toronto; Macquarie University; Edinburgh Napier University; University of Alberta; and British University, Dubai. During his M.Sc. degree, he graduated as the Third Best Student from Islamic Azad University. He has authored and coauthored more than 40 papers in international journals in Nature, IEEE, Elsevier, Springer, T&F, and IEEE conferences. His research interests include complex systems, big data, computational intelligence, artificial intelligence, machine learning, and deep learning. He was successful in receiving several prestigious awards such as the Distinguished Researcher Award for the Best Researcher of Engineering Departments at IAU (Kermanshah, Iran, 2016), the Second Place at the Sixth International Robotic Competitions of the International Federation of Robot Sports Association (FIRA) at the Amirkabir University of Technology in 2016, the First Place at the National Robotics Open Competition of Kurdistan, the Third Place of the Best Ambassador of Power Electronics and Motion Control Competition at 2020 IEEE 19th International Power Electronics and Motion Control Conference, and the Best Presenter in Telecommunication Systems Session at 2021 IEEE 12th Annual Ubiquitous Computing, Electronics and Mobile Communication Conference, New York, USA. Moreover, he has served as a Reviewer with more than 80 reviews for WOS journals and IEEE conferences, such as *Scientific Reports*, IEEE TRANSACTIONS ON INDUSTRIAL INFORMATICS, IEEE ACCESS, *Artificial Intelligence Review*, *Journal of Energy Storage*, *Applied Soft Computing* Journal, and *International Journal of Computer Vision*.

**FARIBORZ PARANDIN** received the B.Sc. and M.Sc. degrees in electrical engineering from the University of Razi, Kermanshah, Iran, in 2000 and 2002, respectively, and the Ph.D. degree in optoelectronic from Razi University, in 2017. He is currently an Assistant Professor of electrical engineering with Islamic Azad University, Kermanshah Branch. His research interests include optoelectronics, semiconductor lasers, photonic crystals, and photonic integrated circuits.

**STANISLAW SZCZEPANSKI** received the M.Sc. and Ph.D. degrees in electronic engineering from the Gdańsk University of Technology, Poland, in 1975 and 1986, respectively. In 1986, he was a Visiting Research Associate with the Institute National Polytechnique de Toulouse (INPT), Toulouse, France. From 1990 to 1991, he was with the Department of Electrical Engineering, Portland State University, Portland, Oregon, on a Kosciuszko Foundation Fellowship. From August to September 1998, he was a Visiting Professor with the Faculty of Engineering and Information Sciences, University of Hertfordshire, Hatfield, U.K. He is currently a Professor with the Department of Microelectronic Systems, Faculty of Electronics, Telecommunications and Informatics, Gdańsk University of Technology. He has published more than 160 papers and holds three patents. His teaching and research interests include circuit theory, fully integrated analog filters, high-frequency transconductance amplifiers, analog integrated circuit design, and analog signal processing.